ELSEVIER

Flow Measurement and Instrumentation 13 (2002) 265–270

Flow Measurement and Instrumentation

www.elsevier.com/locate/flowmeasinst

Non-contact flood discharge measurements using an X-band pulse radar (I) theory

Ming-Ching Lee [a,*], Chan-Ji Lai [a], Jan-Mou Leu [a], William J. Plant [b], William C. Keller [b], Ken Hayes [b]

[a] *Department of Hydraulic and Ocean Engineering, Cheng-Kung University, Tainan 70101, Taiwan*
[b] *Applied Physics Laboratory, University of Washington, Seattle, WA, 98105, USA*

Abstract

This article describes a non-contact method for measuring surface velocity and discharge in a natural channel. The X-band pulse (9.36 GHz) radar, developed by the Applied Physics Laboratory of the University of Washington, was used to scan instantaneously the lateral distribution of surface velocity across a river section, according to Bragg scattering from short waves produced by turbulent boils on the surface of the river. Based on the assumption that the vertical velocity distribution follows a universal power or logarithmic law, the discharges were estimated.

Keywords: Discharge; X-band pulse radar; Turbulent boils

1. Introduction

Flood discharge at a high river stage is important in determining the design of flood-alleviating schemes. Discharge, however, is difficult to measure because high floods usually occur under extreme weather conditions. During flooding, the flow velocity is typically high, for example, above 4 m/sec, and the conventional contact measuring methods can be dangerous for both the persons and the equipment performing the measurements. The search for a non-contact method of flood measurement has been important to hydrologists and hydraulic engineers.

Advances in remote sensing and data processing techniques have yielded great progress in non-contact discharge measurement. This progress follows mainly from the developments of schemes for detecting surface velocity. Imaging process techniques such as the aerial photographic method of Fukuoka et al. [1] and the particle image velocimetry (PIV) of Fujita et al. [2] have been used to measure the surface velocity in rivers. However, the use of VHF radar(s) is a long-established method of measuring water surface currents, as applied by Estournel et al. [3]. However, this method is not suited to most inland river flow measurement, because of its 1 km spatial resolution. Only recently has the X-band Real Aperture Radar been develop at the Applied Physics Laboratory (APL), University of Washington, with a spatial resolution of 3.75–30 meters. It has been used to collect surface velocity data from the Skagit river, WA., as reported by Costa et al. [4]. Subsequently, those researchers translated the data into mean velocities (surface velocity times 0.85) and cross-sectional discharge. They reported that the discharge values agreed well with the values obtained by the traditional contact method. Although the APL X-band radar has proven to be useful in detecting surface velocity, it has not been tested under extreme weather conditions. Moreover, water depth measurements must be taken separately, limiting the usefulness of the technique under difficult weather condition.

2. Estimating water depths and discharge

During an extreme flood event, the depths of a river cross-section change with water stage, and are difficult

* Corresponding author. Tel.: +886 6 2757575 ext. 63268; fax: +886 6 2741463.
E-mail address: n8886102@ccmail.ncku.edu.tw (M.-C. Lee).

0955-5986/02/$ - see front matter © 2002 Elsevier Science Ltd. All rights reserved.
PII: S0955-5986(02)00048-1

Nomenclature

A	empirical coefficient;
B	river width;
a	coefficient of power law;
F_r	Froude number;
g	gravitational acceleration;
h	flow depth;
k_s	roughness height;
m	exponent or power;
Q	river discharge;
s_0	river-bed slope;
s_w	water surface slope;
s_e	energy slope;
u	local velocity at position in river;
$\bar{u}_I$	the inner region average velocity;
$\bar{u}_O$	the outer region average velocity;
u_s	surface velocity in river;
u_*	friction velocity;
V_n	line-of-sight velocity;
x	longitudinal coordinate;
y	lateral coordinate;
z	vertical coordinate; the distance from bed;
z'	characteristic distance from bed;
z_0	range of outer region;
α	transformation coefficient;
κ	Kărman's constant;
Π	Coles wake parameter;
ν	kinematic viscosity of water;
λ_B	Bragg resonant wavelength;
ϕ	azimuth.

to measure. A convenient method must be used to estimate both the water depths and mean velocity of the cross-section. The highly turbulent nature of the flood flow, as described by Kuroki and Kishi [5], Itakura et al. [6] and Kinoshita [7], helps with the estimates, if the vertical velocity profile can be assumed to follow the universal velocity law.

As shown in Fig. 1(a), the width of a working river section at y is B(y). The water surface velocity, sensed by the radar at a position y from the left bank is $u_s(x,y)$, where the water depth is $h(x,y)$. The turbulent flow of a fluid in a open channel can be determined, if the vertical velocity profile follows the universal law, which dictates that the velocity $u(x,y,z)$ or u at a distance z from the channel bed is given by Chen [8],

$$\frac{u}{u_*} = a\cdot\left(\frac{z}{z'}\right)^m, \quad z' = \gamma k_s, \quad a = A(1+m)\nu^m, \tag{1}$$

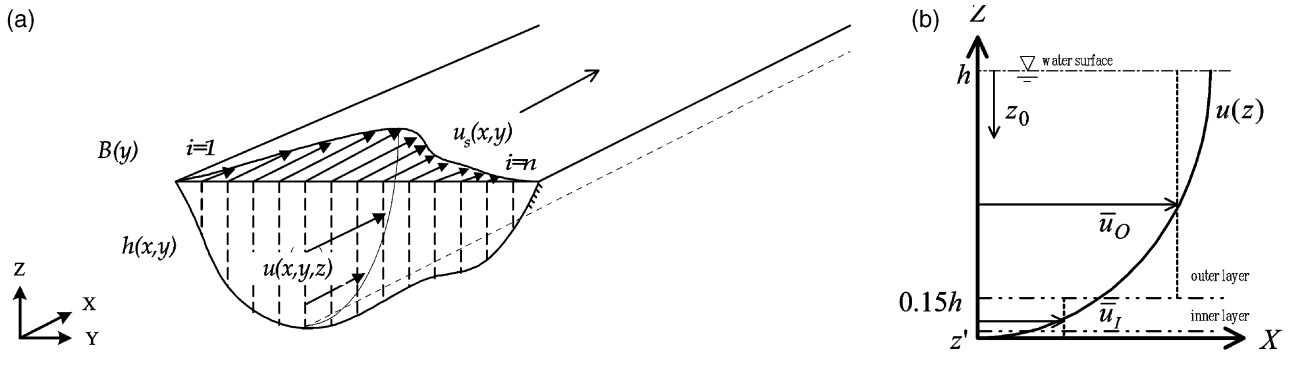

Fig. 1. (a) The lateral distributions of surface velocity and depth (b) velocity profile at vertical.

in which, $u_* = \sqrt{ghs_e}$ is the friction velocity; s_e is the energy slope; z' is the characteristic distance from the river bed and k_s is roughness height; m is the exponent and the coefficient; A is the empirical coefficient. Nikuradse [9] pointed out that $\gamma = 1/30$ in a rough riverbed. From Eq. (1), the relationship between the surface velocity and the water depth is,

$$h = \left(\frac{u_s k_s^m}{A(1+m)\sqrt{gs_e}}\right)^{\frac{2}{2m+1}}. \tag{2}$$

The Manning–Strickler formula determines the values of m and A: $m = 1/6$, $A = 7.68$ [10], but, by Engelund's formula, $m = 1/8$, $A = 9.45$ [11]. Further investigation revealed that the former equation can be used in a gravel river and the latter fits the velocity profiles for a river with deep water or small bed materials.

Furthermore, the velocity profile is expected to follow the logarithm law, as shown Fig. 1(b). In the outer region, $z/h > 0.15$, Coleman and Alonso [12] expressed the wake law as,

$$\frac{u_s - u}{u_*} = \frac{-1}{\kappa}\ln\frac{z}{h} + \frac{2\Pi}{\kappa}\cos^2\left(\frac{\pi z}{2h}\right) \tag{3}$$

where $\kappa = 0.4$ is Karman's constant; Π is Coles' wake parameter. Nezu and Rodi [13] experimentally determined that if $\mathrm{Re} > 10^5$, then $\Pi = 0.2$ as a closed constant. In the inner region, $z/h < 0.15$, and u is expressed as,

$$\frac{u}{u_*} = \frac{1}{\kappa}\ln\frac{z}{z'}. \tag{4}$$

Averaging the velocity throughout the outer and inner region, the regional average velocities, $\bar{u}_o$ and $\bar{u}_I$, are obtained as,

$$\frac{u_s - \bar{u}_o}{u_*} = \frac{1}{\kappa}\cdot\frac{h-z_0}{z_0}\ln\frac{h-z_0}{h} + \frac{1}{\kappa}\left[1 + \Pi - \frac{\Pi h}{\pi z_0}\sin\frac{\pi(h-z_0)}{h}\right] \tag{5}$$

and,

$$\frac{\bar{u}_I}{u_*} = \frac{1}{\kappa}\left[\ln\left(0.15\frac{h}{\nu\cdot k_s}\right) - 1\right] \tag{6}$$

where $z_0 = 0.85h$. Consequently, the vertical average velocity $\bar{u}$ is:

$$\bar{u}_i = 0.15\bar{u}_{I_i} + 0.85\bar{u}_{O_i} \tag{7}$$

where the suffix i refers part of the river section, divided into n parts, $n = 1$ to i, so the river discharge, Q, is,

$$Q = \int_0^B (\bar{u}\cdot h)dy \approx \sum_{i=1}^{n} [\bar{u}_i\cdot h_i\cdot \Delta B_i]. \tag{8}$$

Eq. (8) gives the desired discharge under normal flow conditions if the energy slope is evaluated from the water level and the bed slope. However, the energy slope varies with the water stage during a flood and its value must be determined. If the upstream and downstream water surface velocities are known, then,

$$s_e = s_w - \frac{\bar{u}\partial\bar{u}}{g\partial x} \tag{9}$$

in which s_w is the slope of the water surface. The water depth and the flood discharge can thus be estimated from Eqs. (2) and (8).

3. Measuring surface velocity using radar

The short crest surface waves, which may be generated by wind or channel turbulence, run congruously with the underlying water. The radar backscatters of the resonant Bragg-scattering, at an angle of incidence from these surface waves near the grazing angle, and whose wavelength related to the radar wavelength, produce Doppler shifts if the waves run at certain velocities. The APL microwave Doppler radar, called CORAR (for Real Aperture Radar), was used in this present study. It was a coherent pulse X-band (9.360 GHz) radar, with a pulse width of 25 ηsec, a spatial resolution of 3.75 meters and a Bragg resonant wavelength λ_B of 3 centimeters. The measurements were taken with a parabolic antenna of 60 centimeters in diameter, and that provided a range resolution of about 13 meters at a distance of 200 meters at the incident angles used. The software associated with the system received pulses from up to 100 range bins sufficiently rapidly to perform pulse averaging followed by Fourier transforming at each range bin without aliasing. The analysis software also provided tools for choosing the optimum grazing angle and filing the analyzed Doppler shift and the corresponding surface velocity at each range bin.

The velocity is assumed to be equal in a finite rectangle region shown as Fig. 2(a), to obtain the flow direction, such that $u' = u_1' = u_2'$, $v' = v_1' = v_2'$, yielding u', v' as,

$$u' = -\frac{V_{n1} + V_{n2}}{2\cos(\Delta\phi/2)} \tag{10}$$

$$v' = \frac{V_{n1} - V_{n2}}{2\sin(\Delta\phi/2)} \tag{11}$$

in which V_n are the line-of-sight velocities; $\Delta\phi = \phi_2 - \phi_1$ is the difference between the azimuthal angles, and ϕ_1, ϕ_2 are azimuths.

Transforming coordinates yields,

$$u_s = v'\cos\left(\frac{\phi_1 + \phi_2}{2}\right) + u'\sin\left(\frac{\phi_1 + \phi_2}{2}\right) \tag{12}$$

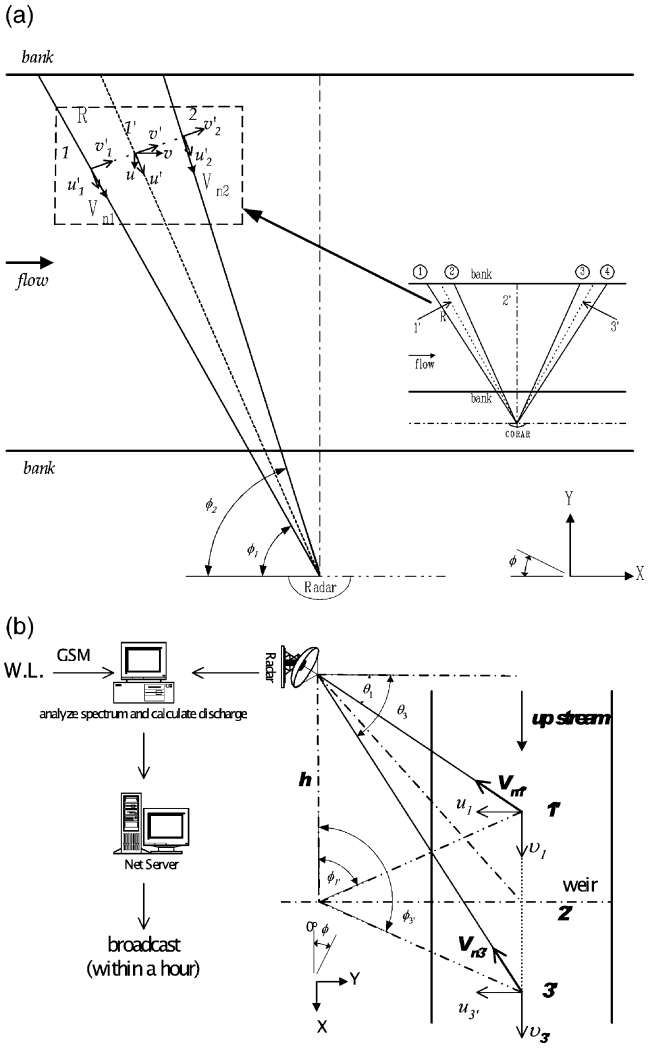

Fig. 2. Vectorization of the currents and the coordinate system in a river using a single radar, (d) Depiction of measuring the river by an automatic Radar system; h is the height of the radar position from the water surface; θ is the incident angle; ϕ is the azimuth.

$$v_s = v'\sin\left(\frac{\phi_1 + \phi_2}{2}\right) - u'\cos\left(\frac{\phi_1 + \phi_2}{2}\right) \tag{13}$$

Rearranging Eq. (10) to (11), (12), (13), yields the surface vector currents u_s, v_s:

$$u_s = \frac{V_{n1}\cos\phi_2 - V_{n2}\cos\phi_1}{\sin(\phi_2 - \phi_1)} \tag{14}$$

$$v_s = \frac{V_{n1}\sin\phi_2 - V_{n2}\sin\phi_1}{\sin(\phi_2 - \phi_1)} \tag{15}$$

Eq. (14) and (15) determine the surface currents, using a single radar, by rotating the radar by a small angle, when the variation of velocities within the angle is small. Fig. 2(b) depicts how the radar was operated at the station, and the river discharges can be easily obtained by measuring the velocity distributions of sections 1–3.

4. Theory verification

Study 1 used an independent data set of Yamaguchi and Niizato [14] were used to verify the above method. Yamaguchi and Niizato used a CW radar and took pointwise surface velocity measurements, assuming that the river flow was in a steady state. Fig. 3(a) and the solid line in Fig. 3(b) show the measured velocities and bed elevation. Assuming that the energy slope equals the bed slope, Fig. 3(b) compares the cross-section deduced from Eq. (2), using Manning–Strickler's and Engelund's formulae ($m = 1/6$, $A = 7.68$; $m = 1/8$ and $A = 9.45$) .The results are good except at locations close to the bank. This deviation may be due to the ignorance of boundary effects, such as the difference of bed roughness, or small eddies near boundary.

Study 2 tested the accuracy of the new X-band radar system when applied to the Zewen River, Taiwan, and compared it to that of the current meter and float method and the PIV scheme (cross-correlation technique). In these experiments, the measured section was situated at the outlet of a power-station. According to the records of the power-station, the discharge decreased from 51 m^3/sec to 36 m^3/sec within an hour, and the average value was 44 m^3/sec. The radar system and the PIV scheme scan the velocity distributions synchronously on the water surface, but the current meter and float method takes only a single point in a single moment. Fig. 4 shows the surface velocity measured by the above four techniques. The values obtained by the float method are smaller than those obtained by the other techniques, because the course of the float can't maintain sufficiently to keep on a line on the water surface. Furthermore, the mean deviation of the velocity values between the radar and PIV measurements is 10.4%. However, the errors associated with the PIV scheme depend on many variables, including image distortion, seeding density and any interpolation procedure, and are between 5 and 10%, or much more for a field measurement. Comparing the measurements of the current meter and float method to those obtained by the radar system, the deviation of the velocity values is 4.5 and 10%, respectively.

Fig. 5 shows the water depths and discharges deduced from Eq. (2) to (3), (4), (5), (6), (7), (8), (9). The interval between the two measurements was 11 minutes. The measured discharges were 43.2 and 38.7 m^3/sec, very close to the records of the power-station. It shows that the radar system can thus measure unsteady flow.

5. Conclusions

River discharge was accurately estimated by logarithm and power formula, by considering surface velocity distribution, obtained by the radar system. The effectiveness of X-band radar in remotely sensing the surface

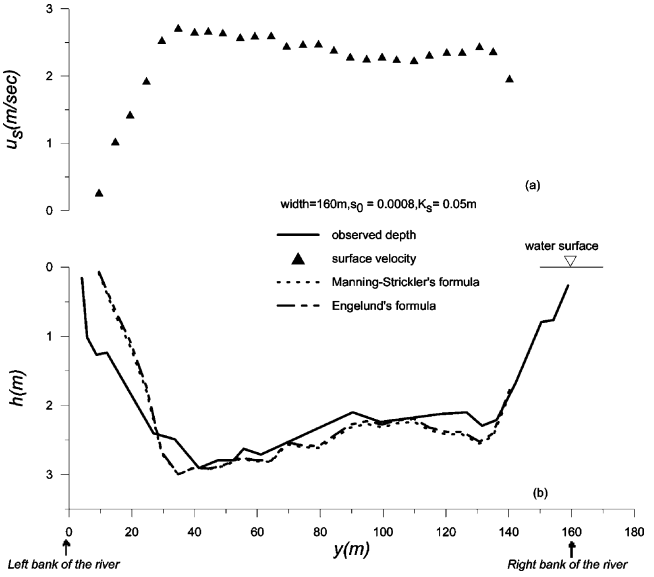

Fig. 3. Comparisons of calculated and measured riverbed profiles in the Unon river. Dots line Manning–Strickler's formula and dashed line the Engelund formula. Steady state is assumed and bed slope is used as the energy slope.

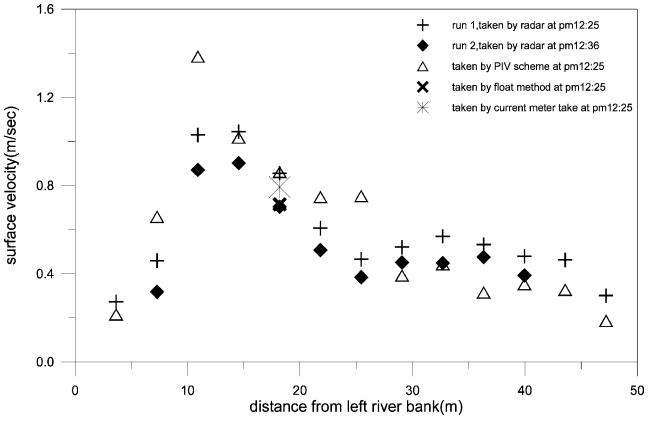

Fig. 4. Comparisons of the velocity values were measured using the radar system, PIV scheme, float method and current meter.

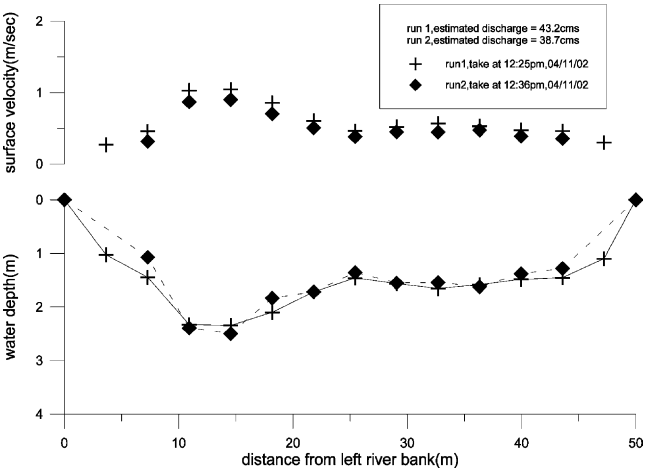

Fig. 5. The cross-sectional depth is deduced from Eq. (2), and there is an interval of 11 minutes between the two measurements. According to the records of the power-station, the discharge was decrease from 51 m^3/sec to 36 m^3/sec within an hour, and the average value was 44 m^3/sec.

velocity in a river and river discharge was examined. Surface velocity measurements, obtained using X-band radar and the current meter, the float method, and the PIV scheme, were closely compared, and the deviation was close to 10%. The remote sensing technique was proven to be very effective and versatile.

For simplicity, variations of lateral velocity distributions are commonly neglected when measuring discharge during flooding, but this simplification yields inaccuracy. Nevertheless, more accurate discharge measurements of lateral velocity variations than taken using the radar system, can be obtained. Moreover, monitoring and measuring flood discharge is impossible under extreme weather conditions, except using a rating curve. However, it is practical to do that using the radar system in this paper.

Acknowledgements

The co-research is financed under the Agreement #122153 of UW and NCKU Hyd and Ocean R&D Foundation. It is also financed by Water Resource Bureau under the contracts:MOEA/WRB-890068 and MOEA/WRB-890032.

References

[1] S. Fukuoka, K. Fujita, T. Araki, Improvement of aerial survey technique for analysis of flood flow, in: Proceedings 32nd Japanese Conference on Hydraulics, 1988, pp. 295–300.

[2] I. Fujita, M. Muste, A. Kruger, Large-scale particle image velocimetry for flow analysis in hydraulic engineering applications, Journal of Hydraulic Research 36 (3) (1998) 397–414.
[3] C. Estournel, P. Broche, P. Marsaleix, J.-L. Devenon, F. Auclair, R. Vehil, The Rhone river plume in unsteady conditions: numerical and experimental results, Estuarine, Coastal and Shelf Science 53 (2001) 25–38.
[4] J.E. Costa, K.R. Spicer, R.T. Cheng, F.P. Haeni, N.B. Melcher, E.M. Thurman, W.J. Plant, W.C. Keller, Measuring stream discharge by non-contact methods: A proof-of-concept experiment, Geophysical Research Letters 27 (4) (2000) 553–556.
[5] M. Kuroki, T. Kishi, Study on the changes of flow resistance and sand waves in Ishikari River, in: Proceedings 27th Japanese Conference on Hydraulics, 1983, pp. 747–752.
[6] T. Itakura, H. Yamaguchi, Y. Shimizu, et al. Observations of Bed P3 Topography during the 1981-August flood in the Ishikari River, in: Proceedings 30th Japanese Conference on Hydraulics, 1986, pp. 481–486.
[7] R. Kinoshita. Observation of alluvial activity during flooding and experiment study on optimum double-section river channel, a special scientific study on natural disasters, subsidized by the ministry of education, 1988, No. A-62-1.
[8] C.L. Chen, Power formula for open-channel flow resistance, in: Proceedings of the 1988 National Conference on Hydraulic Engineer, ASCE, 1988, pp. 25–35.
[9] J. Nikuradse. Gestzmassigkeiten der turbulenten Stromung in glatten Rohren, Ver. Deut. Ing. , Forschungsheft 356, 1932 [in German].
[10] K. Strickler. Beiträge Zur Frage der Geschwindigkeitsformel und der Raukigeitszahlen Fur Strom Kanäle und Geschlossene Leitungen, Mitteilung No. 16 des Eidenőssische Amtes fur Wasser Wirtschaft, Bern, Switzerland, 1923.
[11] F. Engelund, E. Hansen, A Monograph on Sediment Transport in Alluvial Streams, Teknisk Forlag, Copenhagen, 1972 p. 62.
[12] N. Coleman, C.V. Alonso, Two-dimensional channel flows over rough surface, Journal of Hydraulic Engineer, ASCE 109 (2) (1983) 175–188.
[13] I. Nezu, W. Rodi, Open-channel flow measurement with a laser doppler anemometer, Journal of Hydraulic Engineering 112 (5) (1986) 335–355.
[14] T. Yamaguchi, K. Niizato. Flood discharge observation using radio current meter, Doboku Gakkai Rombun-Hokokushu Proceedings of the Japan Society of Civil Engineers, No. 497, 1994, pp. 41–50.